Scientific Report

TRANSPARENT PROCESS

EMBO reports

Genome-wide screen identifies a novel p97/CDC-48-dependent pathway regulating ER-stress-induced gene transcription

Esther Marza[1,2,3], Saïd Taouji[1,2,†], Kim Barroso[1,2,†], Anne-Aurélie Raymond[2,4,†], Léo Guignard[2,3], Marc Bonneu[2,5], Néstor Pallares-Lupon[1,2], Jean-William Dupuy[2,5], Martin E Fernandez-Zapico[6], Jean Rosenbaum[2,4], Francesca Palladino[7], Denis Dupuy[2,3] & Eric Chevet[1,2,8,*]

Abstract

The accumulation of misfolded proteins in the endoplasmic reticulum (ER) activates the Unfolded Protein Response (UPR^{ER}) to restore ER homeostasis. The AAA^+ ATPase p97/CDC-48 plays key roles in ER stress by promoting both ER protein degradation and transcription of UPR^{ER} genes. Although the mechanisms associated with protein degradation are now well established, the molecular events involved in the regulation of gene transcription by p97/CDC-48 remain unclear. Using a reporter-based genome-wide RNAi screen in combination with quantitative proteomic analysis in *Caenorhabditis elegans*, we have identified RUVB-2, a AAA^+ ATPase, as a novel repressor of a subset of UPR^{ER} genes. We show that degradation of RUVB-2 by CDC-48 enhances expression of ER stress response genes through an XBP1-dependent mechanism. The functional interplay between CDC-48 and RUVB-2 in controlling transcription of select UPR^{ER} genes appears conserved in human cells. Together, these results describe a novel role for p97/CDC-48, whereby its role in protein degradation is integrated with its role in regulating expression of ER stress response genes.

Keywords AAA^+ ATPase; proteostasis; UPR
Subject Categories Protein Biosynthesis & Quality Control
DOI 10.15252/embr.201439123 | Received 4 June 2014 | Revised 21 December 2014 | Accepted 2 January 2015 | Published online 4 February 2015
EMBO Reports (2015) 16: 332–340

Introduction

The endoplasmic reticulum (ER) protein quality control system ensures the correct folding of transmembrane and secretory proteins before their export from this organelle [1]. Accumulation of improperly folded proteins in the ER triggers the unfolded protein response (UPR^{ER}) to restore ER homeostasis. This is achieved by enhancing ER-Associated Degradation (ERAD), increasing ER protein folding capacity, decreasing protein translation and inducing a defined gene expression profile (UPR^{ER} genes) [2]. Although most of these molecular events are clearly established, the mechanism leading to the transcriptional regulation of specific genes under ER stress remains poorly understood.

Here, using as a model the nematode *C. elegans*, we identify a novel functional partner for p97/CDC-48, an AAA^+ ATPase involved ER stress response, in the regulation of ER-stress-associated UPR^{ER} gene transcription. *C. elegans* expresses two p97/CDC-48 homologs, *cdc-48.1* and *cdc-48.2*, which share similar functions in ERAD. While simultaneous silencing of both *cdc-48.1* and *cdc-48.2* leads to ER stress, UPR^{ER} gene activation and lethality [3]. Inactivation of either *cdc-48.1* or *cdc-48.2* is viable but abolishes the transcriptional activation of UPR^{ER} genes in response to ER stress [4]. Using a *C. elegans* strain mutant for the p97/CDC-48 homolog $cdc\text{-}48.2^{(-/-)}$, we performed a genome-wide RNAi screen to identify proteins involved in the activation of UPR^{ER} genes during ER stress. We found that the AAA^+ ATPase RUVB-2 is a regulator of the ER stress response by repressing the transcription of select UPR^{ER} genes in non-stressed conditions in both *C. elegans* and human cells. In response to ER stress, RUVB-2 is degraded in a CDC-48-dependent manner, thereby relieving repression of UPR^{ER} genes. Altogether, our results identify a novel mechanism controlling gene expression downstream of p97/CDC-48 and unveil a novel function for RUVB-2 and its human homolog Reptin as a key regulator of the transcriptional response to ER stress.

1 Team "Endoplasmic Reticulum stress and cancer", INSERM, UMR1053, Bordeaux, France
2 University of Bordeaux, Bordeaux, France
3 ARNA laboratory, INSERM U869, Bordeaux, France
4 "REPTeam", INSERM, UMR1053, Bordeaux, France
5 Plateforme Proteome, Bordeaux, France
6 Schulze Center for Novel Therapeutics, Division of Oncology Research, Mayo Clinic, Rochester, MN, USA
7 Laboratory of Molecular and Cellular Biology, Ecole Normale Supérieure, CNRS UMR5239, Université de Lyon, Lyon Cedex 07, France
8 Centre Régional de Lutte Contre le Cancer Eugène Marquis, Rennes, France
*Corresponding author. Tel: +33 557579253; E-mail: eric.chevet@inserm.fr
†These authors contributed equally to this work

Results and Discussion

A genome-wide screen identifies *cdc-48* genetic interactors regulating ER-stress-induced gene expression

RNAi-mediated knockdown of *cdc-48.1* or *cdc-48.2* in *C. elegans* abolishes the ER-stress-induced expression of a set of UPR^{ER} genes including *ckb-2* [4]. Using a transcriptional reporter expressing GFP under the control of the *ckb-2* promoter, we confirmed the requirement for *cdc-48.1* and *cdc-48.2* in ER-stress-induced gene transcription (Fig 1A). Mutant *cdc-48.1*$^{(-/-)}$ and *cdc-48.2*$^{(-/-)}$ worms failed to respond to the ER-stress inducer tunicamycin while *ckb-2p::gfp* fluorescence was increased more than threefold in wild-type (WT) worms (Fig 1B). RNAi inactivation of *ire-1*, the main sensor of ER stress and mediator of UPR^{ER} signaling, resulted in a significant decrease in fluorescence intensity in both *ckb-2p::gfp* and *cdc-48.2*$^{(-/-)}$; *ckb-2p::gfp* worms (Fig 1A, Supplementary Table S1). These results confirm that *ckb-2p::gfp* transcription is IRE1 dependent, as expected of a *bona fide* UPR^{ER} reporter.

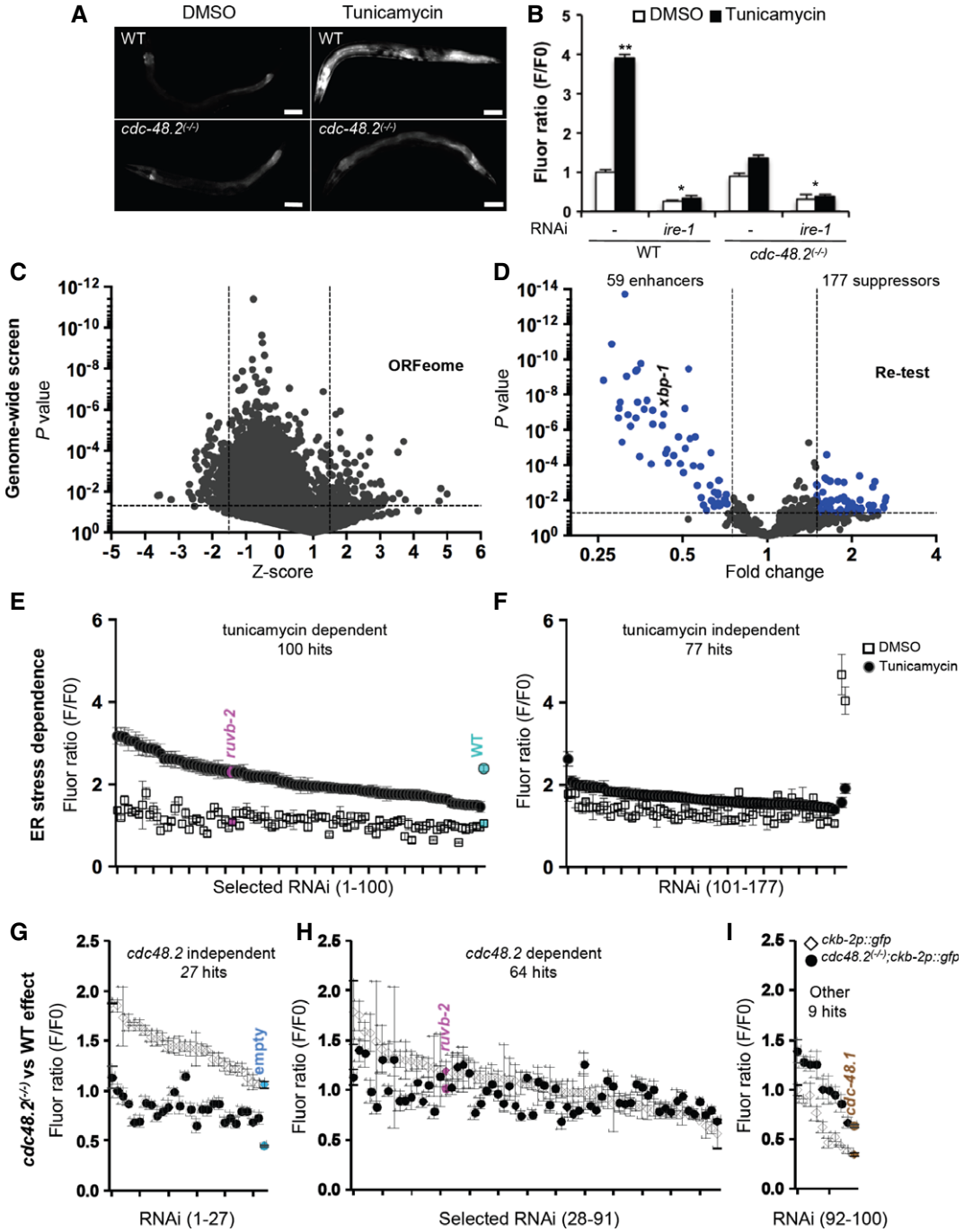

Figure 1.

Because p97/CDC-48 is involved in protein degradation [5], we reasoned that it might modulate ER-stress-induced *ckb-2p* transcription by eliminating a transcriptional repressor. To address this hypothesis, we designed an RNAi suppressor screen to identify genes whose knockdown could restore tunicamycin *ckb-2p::gfp* activation following ER stress in a *cdc-48.2*$^{(-/-)}$ mutant background ([4]; Fig 1C). We performed the screen in liquid culture by feeding *cdc-48.2*$^{(-/-)}$; *ckb-2p::gfp* synchronized L1 larvae with double-stranded RNA (dsRNA)-expressing *E. coli* derived from the *C. elegans* ORFeome library that targets 11,698 open reading frames covering 62% of *C. elegans* genes [6]). We then exposed the worms to a concentration of tunicamycin (0.5 μg/ml for 16 h) leading to maximal *ckb-2p::gfp* induction in WT worms grown in liquid culture and analyzed them by flow cytometry [7] to measure their length, number and fluorescence intensity. Each RNAi clone was tested in duplicate, and the mean *Z*-score was calculated. Two-hundred and forty-one RNAi clones synergized with *cdc48.2*$^{(-/-)}$ to decrease *ckb-2p::gfp* expression in our primary screen (mean *Z*-score value less than −1.5, or one of the two independent *Z*-scores less than −3) (Fig 1C). Of these, 59 clones significantly decreased GFP fluorescence below 0.75-fold ($P < 0.05$) (Fig 1D, Supplementary Table S2). One-hundred and seventy-seven RNAi clones instead reproducibly increased (average *Z*-score >1.5 or one of the two individual *Z*-scores >3) GFP fluorescence 1.5-fold above the fluorescence intensity measured with *cdc-48.2*$^{(-/-)}$; *ckb-2p::gfp* worms fed with an empty vector and treated with tunicamycin ($P < 0.05$). These were classified as potential suppressors of the *cdc48.2*$^{(-/-)}$ phenotype.

To discriminate between ER-stress-dependent and ER-stress-independent activation of *ckb-2p::gfp* transcription, we measured fluorescence intensity in *cdc-48.2*$^{(-/-)}$; *ckb-2p::gfp* worms fed with candidate RNAi clones and treated either with tunicamycin or vehicle (DMSO; Fig 1E). Seventy-seven RNAi clones showing a similar increase in the fluorescence ratios under both conditions were considered ER-stress independent and not further analyzed (Fig 1F, Supplementary Table S3). By contrast, 100 RNAi clones which restored *ckb-2p::gfp* activation in the *cdc48.2*$^{(-/-)}$ mutant background specifically under tunicamycin treatment were identified as ER-stress-dependent suppressors of *cdc48.2*$^{(-/-)}$ (Fig 1E, Supplementary Table S4). We next investigated whether the genes targeted by these RNAi clones could activate gene transcription specifically under ER stress independently of *cdc-48.2*. If a targeted gene acts exclusively in the same genetic pathway as *cdc-48.2*, then its knockdown by RNAi should not increase *ckb-2p::gfp* transcription in a WT background, nor have an additive effect with the *cdc-48.2*$^{(-/-)}$ mutation on *ckb-2p::gfp* transcription. We quantified and compared *ckb-2p::gfp* fluorescence intensities in both WT and *cdc-48.2*$^{(-/-)}$ mutant worms fed with RNAi and exposed to tunicamycin. Twenty-seven RNAi clones increased fluorescence intensities in WT more than in *cdc-48.2*$^{(-/-)}$ worms (fold change ≥1.4, Fig 1G). Nine other clones showed higher fluorescence in mutant worms compared to WT (fold change ≥1.4, Fig 1I), similar to *cdc-48.1* RNAi. The corresponding 36 genes (27+9) were therefore not considered as strict suppressor of *cdc-48.2* and were not further analyzed. We thus identified 64 suppressor RNAi clones that did not show any synthetic enhancement phenotype in *cdc-48.2*$^{(-/-)}$ relative to WT (fold change < 1.4 and $P < 0.05$, Fig 1H). Taken together, these results identify genes controlling *ckb-2p::gfp* expression upon ER stress in a CDC-48 dependent fashion and may provide mechanistic insight for the role of CDC-48 in ER-stress-induced gene expression (Fig 2A). Among these candidates, the AAA+ ATPase *Ruvb2* was of particular interest.

To confirm the RNAi screen findings, we conducted a quantitative proteomic analysis to identify proteins whose levels are modified in *cdc-48.2*$^{(-/-)}$; *ckb-2p::gfp* worms exposed to tunicamycin. We selected proteins represented by at least two peptides and that had a peptide ratio above 2 or below 0.5 between WT and mutant worms exposed to tunicamycin. Ninety-three proteins increased and 15 proteins decreased in abundance in *cdc-48.2*$^{(-/-)}$ mutants compared to the WT (Fig 2B, Supplementary Table S5). RUVB-2 was the only suppressor identified in our RNAi screen for which an increase in protein abundance could be detected in *cdc-48.2*$^{(-/-)}$; *ckb-2p::gfp* compared to *ckb-2p::gfp* worms (2.5 ± 0.5-fold increase, Fig 2C).

Figure 1. RNAi screening identifies *cdc-48.2* genetics interactors in the *ckb-2* transcriptional response to ER stress.

A *cdc-48.2* is required to activate *ckb-2p::gfp* transcription in response to tunicamycin. Images of adult worms (left) expressing *gfp* under the control of the *ckb-2* gene promoter in WT (upper panels) and in *cdc-48.2*$^{(-/-)}$ mutants (lower panels) exposed to tunicamycin (5 μg/ml) or DMSO for 16 h. (Scale bar: 50 μm, obj.: 10×).

B Significant changes in fluorescence intensities were quantified using flow cytometry. L1 larvae (*ckb-2p::gfp* and *cdc-48.2*$^{(-/-)}$; *ckb-2::pgfp* larvae) were fed with bacteria expressing the L4440 empty vector or *ire-1* RNAi in liquid culture and exposed to tunicamycin (0.5 μg/ml) or DMSO for 16 h. F0 was defined as the fluorescence intensity obtained in *ckb-2p::gfp* worms fed with the empty vector and treated with DMSO. (Mean ± s.e.m, $N = 8$, 200 worms/experiment). *P*-values were calculated using multiple *t*-test corrected using the Holm–Sidak method $^{**}P < 0.001$; $^{*}P < 0.01$.

C Genome-wide RNAi screen identifies suppressors and enhancers of *cdc-48.2*$^{(-/-)}$ in *ckb-2p::gfp* transcription. Volcano plots present results obtained using *Caenorhabditis elegans* ORFeome library.

D Re-testing of RNAi clones from first round.

E, F Classification of ER stress dependence of the 177 suppressor RNAi clones able to restore *ckb-2p::gfp* transcription in *cdc-48.2*$^{(-/-)}$ mutant background. *cdc-48.2*$^{(-/-)}$; *ckb-2p::gfp* synchronized L1 larvae were fed with the dsRNA expressing bacteria in liquid culture, treated with tunicamycin (0.5 μg/ml) or DMSO for 16 h, and fluorescence intensities were measured by flow cytometry. (E) Tunicamycin-dependent RNAi clones were defined as those that significantly increased fluorescence ratio following tunicamycin treatment (Tunicamycin/DMSO F/F0 fold change > 1.5). (F) Tunicamycin-independent RNAi clones were defined as those increasing *ckb-2p::gfp* fluorescence ratio in both conditions (Tunicamycin/DMSO F/F0 fold change < 1.5, $P > 0.05$). Fluorescence ratios obtained with *ruvb-2* RNAi are shown in magenta. Fluorescence ratios obtained with *ckb-2p::gfp* worms fed with the empty vector and treated with tunicamycin (2.38 ± 0.18) or DMSO (1.05 ± 0.2) are shown in cyan.

G–I F0 was defined as the fluorescence intensity obtained in *cdc-48.2*$^{(-/-)}$; *ckb-2p::gfp* worms fed with the empty vector and treated with tunicamycin or DMSO, respectively. (Mean ± s.e.m, $N = 5$). Identification of ER-stress-dependent RNAi clones targeting genes involved in the same genetic pathway as *cdc-48.2* to increase *ckb-2p::gfp* transcription. Fluorescence ratio were determined on *cdc-48.2*$^{(-/-)}$; *ckb-2::gfp* and *ckb-2::gfp* worms fed with the suppressor RNAi clones and treated with tunicamycin (0.5 μg/ml) for 16 h. Graphs present the RNAi clones whose effect on *ckb-2p::gfp* fluorescence was higher ((G), (*ckb-2::gfp* F/F0/*cdc-48.2*$^{(-/-)}$; *ckb-2::gfp* F/F0) fold change > 1.4-fold), similar ((H), (*ckb-2::gfp* F/F0/*cdc-48.2*$^{(-/-)}$; *ckb-2::gfp* F/F0) fold change < 1.4, $P > 0.05$) or lower ((I), (*ckb-2::gfp* F/F0/*cdc-48.2*$^{(-/-)}$; *ckb-2::gfp* F/F0) fold change < 0.75) in *ckb-2p::gfp* worms compared to *cdc-48.2*$^{(-/-)}$; *ckb-2p::gfp* worms. Fluorescence ratios obtained with *ruvb-2* RNAi and the two controls empty vector and *cdc-48.1* control RNAis are shown in magenta, cyan and brown, respectively. (Mean ± s.e.m, $N = 5$).

A

Process	Sequence Name	Gene Name	Brief description of gene product
Metabolism (lipid)	C24A11.9	*coq-1*	putative hexaprenyl pyrophosphate synthetase
Metabolism (lipid)	C49D10.4	*oac-10*	O-acyltransferase homolog
Metabolism (lipid)	Y42G9A.4	*mvk-1*	orthologous to the human gene MEVALONATE KINASE
Metabolism (lipid)	C52B9.1	*cka-2*	isoform of choline kinase
Metabolism (redox)	C29E4.7	*gsto-1*	thiol oxidoreductase and dehydroascorbate reductase
Metabolism (redox)	F56F10.3	*cdo-1*	cysteine dioxygenase
Metabolism (RNA)	F25H5.6	*mrpl-54*	mitochondrial ribosomal protein, large
Metabolism (RNA)	R74.5	*asd-1*	alternative Splicing Defective
Metabolism (protein)	Y67D8C.5	*eel-1*	Hect E3 ubiquitin ligase t
Metabolism (protein)	F59A3.3	*mrpl-24*	Mitochondrial Ribosomal Protein, Large
Metabolism (protein)	K07C5.7	*ttll-15*	putative tubulin polyaminoacid ligase
Metabolism (protein)	M01F1.1	*gly-14*	N-acetylglucosaminyltransferase I (GlnT1)
Metabolism (protein)	F26D10.10	*gln-5*	glutamine synthetase (glutamate-ammonia ligase)
Signaling	Y47D3B.2	*nlp-21*	neuropeptide-like proteins
Signaling	T02D1.3	*sru-15*	Serpentine receptor, class U
Signaling	T22B7.5	*srv-7*	serpentine receptor, class V
Signaling	ZC204.11	*btb-13*	BTB (Broad/complex/Tramtrack/Bric a brac) domain protein
Signaling	M01G12.1	*sri-14*	serpentine receptor, class I
Signaling	F45C12.10	*math-29*	MATH (meprin-associated Traf homology) domain containing
Signaling	F55A12.3	*ppk-1*	phosphatidylinositol-4-phosphate 5' kinase
Signaling	K07C5.8	*cash-1*	orthologous to Drosophila CKA and the human striatins
Signaling	C04E12.11	*arrd-20*	ARRestin Domain protein
Signaling	F14F3.2	*git-1*	homologous to mammalian G protein-coupled receptor kinase InTeractor 1
Traffic/transport	Y48G1A.3	*daf-25*	C. elegans ortholog of mammalian Ankmy2
Traffic/transport	C06G3.2	*klp-18*	kinesin motor protein
Traffic/transport	C54G10.3	*pmp-3*	putative ABC transporter orthologous to human ABCD4
Traffic/transport	M03F8.2	*pst-1*	orthologous to the PAPST1 transporter
Transcription	K08A2.5	*nhr-88*	nuclear Hormone Receptor family
Transcription	T22D1.10	*ruvb-2*	RUVB (recombination protein) homolog

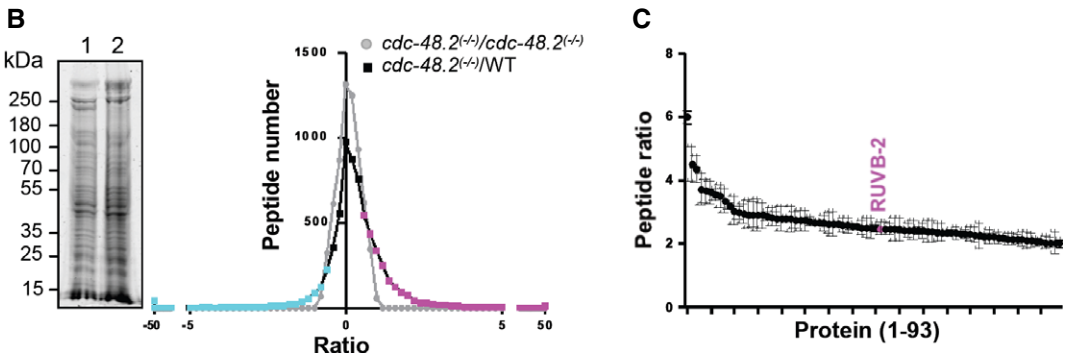

Figure 2. Identification of RUVB2 as a candidate CDC-48 target.

A List of RNAi clones suppressing the *cdc-48.2*$^{(-/-)}$ phenotype.

B Graph representing identified peptide number identified in function of peptide quantity ratio. *cdc-48.2*$^{(-/-)}$*; ckb-2::gfp* and *ckb-2::gfp* synchronized L1 larvae were grown to the L4 stage and exposed to tunicamycin (5 µg/ml) for 16 h on plates. Proteins (60 µg) were separated on a 10% SDS gel. A coomassie blue staining image representative of the SDS gel is shown on the left (1: *cdc-48.2*$^{(-/-)}$*; ckb-2::gfp*, 2: *ckb-2::gfp*). Gel lanes were cut into slices before proteins were in-gel-digested. Peptides were then identified and quantified by label-free LC-MS/MS mass spectrometry. Peptides that were more (magenta) or less (cyan) abundant in the *cdc-48.2*$^{(-/-)}$*; ckb-2::gfp* than in *ckb-2::gfp* worms were defined as those having a ratio above 1.5 or below 0.5, respectively. $N = 3$.

C Graph representing peptide quantity ratio ((*cdc-48.2*$^{(-/-)}$*; ckb-2::gfp)/(ckb-2::gfp)*) for the 93 proteins that are more abundant in *cdc-48.2*$^{(-/-)}$ mutant background compared to WT background. (Mean ± s.e.m, $N = 3$).

Because the quantity of *ruvb-2* mRNA was not increased (Supplementary Fig S4A) under these conditions, the increased abundance of RUVB-2 in *cdc-48.2*$^{(-/-)}$ mutants is likely due to attenuation of protein degradation rather than to increased transcription.

Conserved RUVB-2 and CDC-48-dependent regulation of UPR^{ER} gene expression

RNAi knockdown of *ruvb-2* restored *ckb-2p::gfp* activation both in *cdc-48.2*$^{(-/-)}$ and *cdc-48.1*$^{(-/-)}$ mutant worms exposed to tunicamycin (Fig 3A–B). This suggests that, under ER stress, the repressor RUVB-2 is degraded through a CDC-48.1-dependent mechanism to allow full *ckb-2p::gfp* induction. Moreover, knockdown of *xbp-1* reduced *ckb-2p::gfp* expression in *cdc-48.2*$^{(-/-)}$*; ckb-2p::gfp* worms treated with tunicamycin compared to the DMSO-treated ones (Fig 3C). Combined RNAi-mediated knock-down of *xbp-1* and *ruvb-2* decreased *ckb-2p::gfp* fluorescence to the same level observed using *xbp-1* RNAi alone. This suggests that RUVB-2 is degraded through a CDC-48-dependent mechanism in response to tunicamycin, thus allowing XBP-1s to activate *ckb-2* expression. *Ruvb-2* inactivation also restored the expression of ER homeostasis regulators (CKB-2, F22E5.6, Y71F9AL.17/COPA-1) observed upon ER stress in

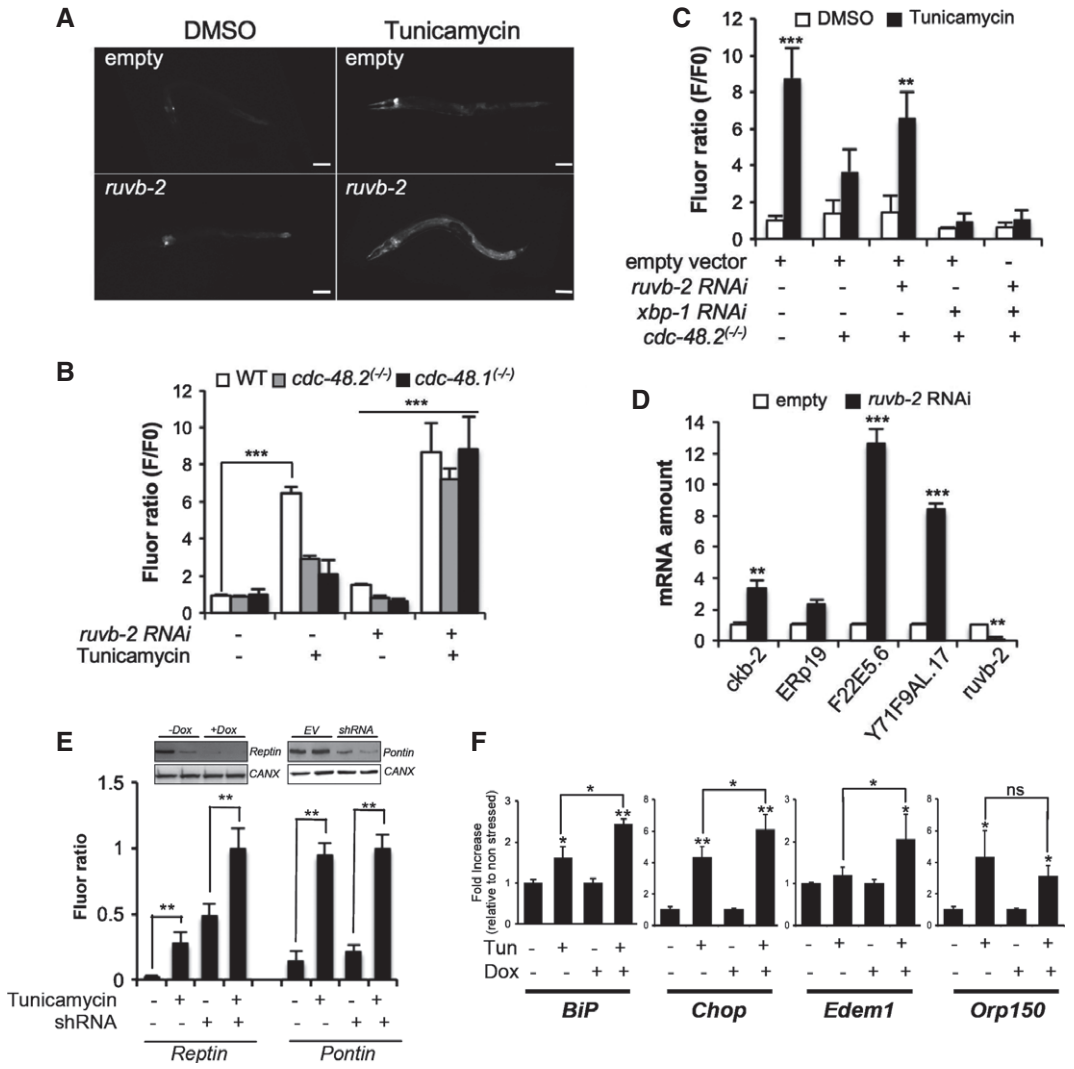

Figure 3. RUVB-2 is a transcriptional repressor inactivated by CDC-48 upon ER stress.

A Images of *cdc-48.2*$^{(-/-)}$*; ckb-2::gfp* adult worms fed with either the L4440 empty vector (upper panel) or *ruvb-2* RNAi (lower panel) and treated with tunicamycin (5 μg/ml) or DMSO for 16 h on NGM agar plates. (Scale bar: 50 μm, obj: 10×).

B Fluorescence was quantified by flow cytometry on *ckb-2::gfp*, *cdc-48.1*$^{(-/-)}$*; ckb-2::gfp* and *cdc-48.2*$^{(-/-)}$*; ckb-2::gfp* worms fed with *ruvb-2* RNAi or empty vector starting at the L1 stage in liquid culture and exposed to tunicamycin (0.5 μg/ml) or DMSO for 16 h. Fluorescence (F) was normalized to the basal fluorescence obtained with empty vector and DMSO in the WT background (F0). (Mean ± SD, $N = 5$) ***$P < 0.001$.

C Fluorescence (F) was quantified by flow cytometry on *ckb-2::gfp* and *cdc-48.2*$^{(-/-)}$*; ckb-2::gfp* worms fed with either *ruvb-2* and empty vector (1:1), *xbp-1* and empty vector (1:1), *ruvb-2* and *xbp-1* RNAi (1:1), or empty vector alone and treated with tunicamycin (0.5 μg/ml) or DMSO for 16 h. Fluorescence (F) was normalized to the basal fluorescence obtained with the empty vector and DMSO in the WT background (F0). (Mean ± s.e.m, $N = 3$). *P*-values were calculated using multiple *t*-test corrected using the Holm-Sidak method. **$P < 0.01$; ***$P < 0.001$.

D RT–qPCR quantification of the relative expression levels of 3 endogenous ER homeostasis genes (ERp19, F22E5.6, Y71F9AL.17/COPA-1), Ckb-2 and Ruvb-2 following tunicamycin treatment in *cdc-48.2*$^{(-/-)}$ worms subjected or not to *ruvb-2* RNAi. Bars represent the mean of three biological replicates. (Mean ± s.e.m, $N = 3$) **$P < 0.01$; ***$P < 0.001$.

E Fluorescence was quantified in HuH7 cells expressing the ERSE::Tomato construct and either the *Reptin* shRNA induced with doxycycline (left) or the Pontin shRNA (transient, right). Cells were exposed to tunicamycin (5 μg/ml) for 4 h prior to measurement. Data are presented as mean ± SD of three independent experiments. Note that Reptin levels were decreased upon Tunicamycin treatment (see also Fig 4A). **$P < 0.01$.

F RT–qPCR analysis of four ER homeostasis control genes under basal conditions or upon tunicamycin treatment (5 μg/ml, 16 h) in HuH7 cells subjected or not to doxycycline-induced *Reptin* silencing. Data are presented as mean ± SD of three independent biological triplicates. (Mean ± s.e.m, $N = 3$) *P*-value was calculated using multiple *t*-test corrected using the Holm-Sidak method. *$P < 0.05$; **$P < 0.01$.

WT animals [8] in *cdc-48.2*$^{(-/-)}$ tunicamycin-treated worms (Fig 3D and Supplementary Fig S4B). These results suggest that RUVB-2 represses the expression of select UPR^{ER} target genes. We next tested whether this function was conserved in human cells. To this end, Huh7 cells transfected with the ER stress response element reporter gene (ERSE::tomato [9]) were knocked down for *Reptin* using stable integration of a doxycycline-inducible short hairpin RNA (shRNA [10]) (Fig 3E, left). Induction of *Reptin* shRNA

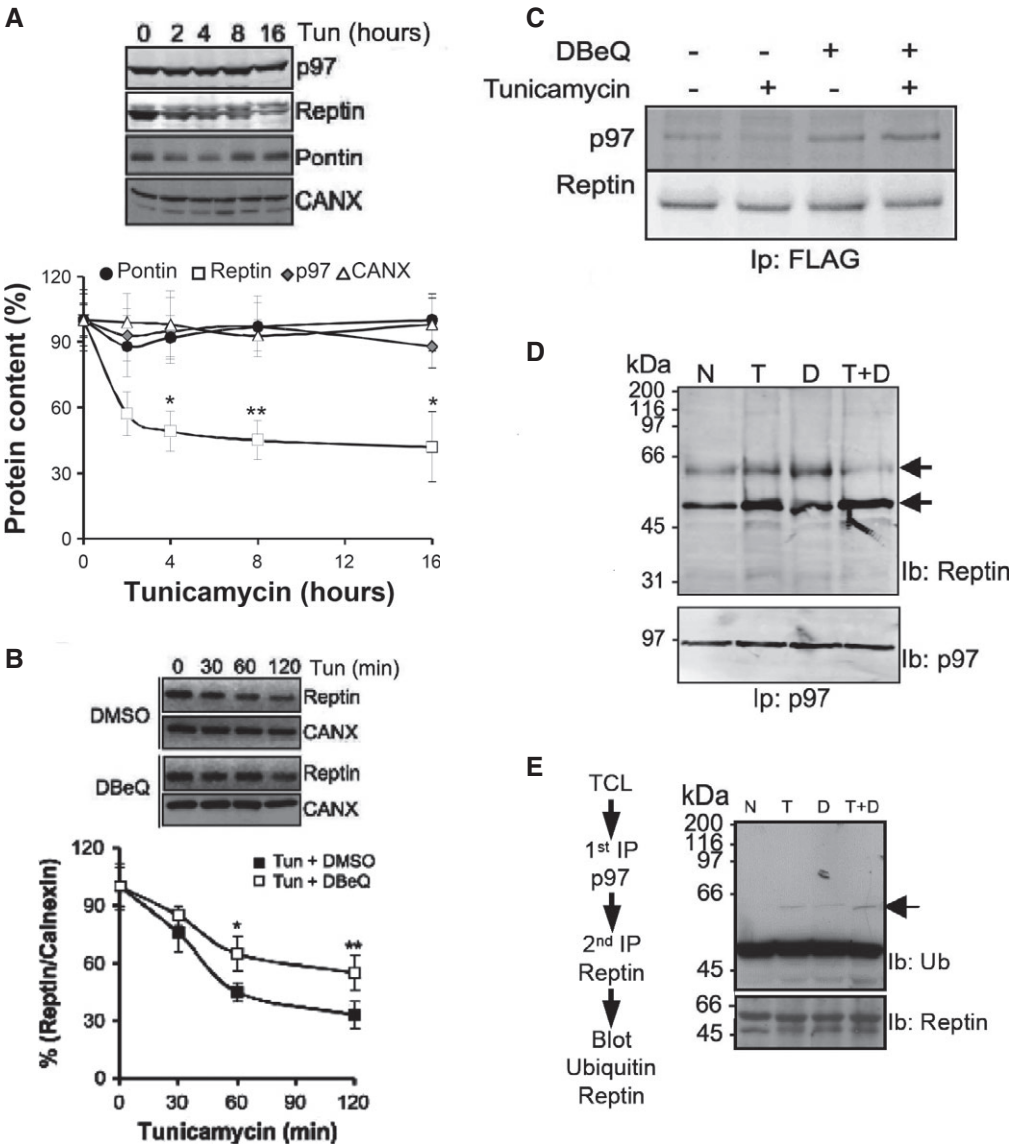

Figure 4. p97/CDC-48-mediated degradation of Reptin upon ER stress.

A Reptin, Pontin, calnexin and quantification by immunoblot. Values are expressed as a percentage of the initial protein abundance in total HuH7 cell lysate before addition of tunicamycin (5 μg/ml), (Mean ± SD, $N = 5$). *$P < 0.05$; **$P < 0.01$.

B Immunoblot analysis of Reptin in total protein extracts from HuH7 cells exposed to tunicamycin (5 μg/ml) for 0–2 h. Protein levels were normalized to Calnexin (mean ± SD, $N = 3$). *$P < 0.05$; **$P < 0.01$.

C HuH7 cells expressing FLAG tagged Reptin were treated either with the p97/CDC-48 inhibitor DBeQ (20 μM, D), the ER stress inducer tunicamycin (2 μg/ml; T) or both for 4 h. FLAG tagged Reptin was immunoprecipitated from total protein extracts using anti-FLAG antibodies, and p97/CDC-48 association was analyzed by immunoblot.

D HuH7 cells were treated either with DBeQ (20 μM, D), (2 μg/ml; T) or both for 4 h. P97/CDC-48 was immunoprecipitated from total protein extracts using an antibody specific for p97/CDC-48, and reptin association was analyzed by immunoblotting.

E HuH7 cells were treated either with DBeQ (20 μM, D), tunicamycin (2 μg/ml; T) or both for 4 h. P97/CDC-48 was immunoprecipitated from total protein extracts using anti-p97/CDC-48 antibodies. P97/CDC-48 immunoprecipitate was disrupted with 50 μl of 1% SDS and heated at 95°C for 5 min. Beads were removed and the supernatant quenched with PBS containing 1% TX-100. Reptin was then sequentially immunoprecipitated and the resulting immunoprecipitate immunoblotted with anti-Ubiquitin or anti-Reptin antibodies.

synergized with tunicamycin treatment to activate ERSE::tomato transcription, demonstrating that Reptin can also a repress ER-stress-mediated transcription in human cells. Of note, the silencing of the Reptin homolog Pontin did not affect the transcription of the ERSE::tomato reporter under basal conditions or upon tunicamycin-induced ER stress (Fig 3E, right). We next quantified the mRNA amounts of 4 genes whose products are involved in the control of ER homeostasis (BiP, CHOP, EDEM1, ORP150). This revealed that Reptin silencing significantly increased the expression of BiP, CHOP and EDEM1 while did not affect that of ORP150

(Fig 3F). Moreover, Reptin overexpression led to the significant repression of select genes (CHOP, EDEM1, ORP150) under basal conditions when compared to control transfected cells (Supplementary Fig S5). Altogether, these results suggest the existence of a conserved role for Reptin in repressing expression of ER stress response genes.

Post-translational control of Reptin expression by p97/CDC-48 impacts on ER stress response in human cells

Further, we examined whether p97/CDC-48 could also acted by triggering the degradation of Reptin in response to ER stress as observed in *C. elegans* (Fig 2). Reptin protein levels were significantly decreased upon tunicamycin treatment, whereas p97/CDC-48, Pontin and Calnexin protein expression remained unaffected (Fig 4A). Conversely, addition of the p97/CDC-48 inhibitor DBeQ stabilized Reptin levels under ER stress (Fig 4B). We then tested whether p97 and Reptin interacted physically using co-immunoprecipitation. These results were confirmed by determining Reptin's half-life upon stress (Supplementary Table S6), and the values obtained under basal conditions were in the range of those determined in *S. cerevisiae* or *S. pombe* [11]. Reptin immunoprecipitates contained p97/CDC-48, and the interaction was modulated by tunicamycin-induced ER stress, DBeQ or both (Fig 4C). Interestingly, when the reverse experiment was carried out, Reptin was found in the p97/CDC-48 immunoprecipitate as well as a slower migrating Reptin immunoreactive species (Fig 4D, arrow). Sequential immunoprecipitation with p97/CDC-48 and Reptin antibodies suggested that the latter corresponds to an ubiquitylated form of Reptin (Fig 4E). Hence, p97/CDC-48 might control Reptin levels through an ubiquitin-dependent mechanism.

XBP1 mRNA splicing and ATF6 activation are partly regulated by a p97/reptin signaling axis

To follow up on the role of Reptin degradation upon ER stress in the expression of ER stress genes, we sought to test whether artificial modulation of Reptin expression also impacted the activation of the three UPR signaling arms. Reptin silencing slightly increased the expression of the ER-stress-upregulated chaperones GRP78 and GRP94, which are canonical targets of ATF6 and XBP1s signaling, under basal conditions (Fig 5A), but did not affect tunicamycin-induced phosphorylation of eIF2α (Fig 5B). ATF6 cleavage activation was increased after Reptin silencing in HuH7 cells (Fig 5C). In accordance with this observation, reptin silencing also enhanced the expression of XBP1u mRNA under basal conditions, as could be expected since XBP1u is a target gene of ATF6 (Fig 5D). Moreover, this occurred without affecting the expression levels of the newly discovered XBP1 mRNA ligase RtcB [12] (Fig 5D). XBP1 mRNA splicing was also increased when Reptin was silenced both in basal conditions and ER stress (Fig 5E). Conversely, DBeQ-mediated p97/CDC-48 inhibition (Fig 5F) or siRNA-mediated p97/CDC-48 silencing (Supplementary Fig S6) and the subsequent stabilization of Reptin led to reduced XBP1 mRNA splicing. Hence, partial stabilization of Reptin has a major impact on XBP1 mRNA splicing, which in turn impacts dramatically on the expression of various UPR^{ER} genes. However, we could not detect an interaction between Reptin and XBP1s protein (Fig 5G). Altogether, these results might indicate that Reptin is degraded through ubiquitin and p97/CDC-48-dependent mechanisms under ER stress and further support the role of Reptin in the control of select UPR^{ER} genes through repression of XBP1 mRNA splicing and of ATF6 activation.

In the present work, we have uncovered a novel regulatory mechanism of UPR^{ER} genes expression in response to ER stress conserved throughout metazoan evolution involving two AAA^+ ATPases, RUVB-2 (or Reptin) and CDC-48 (or p97). In this model, RUVB-2, which mostly localizes to the cytoplasm and the nucleus, plays an important role in the regulation of XBP1 mRNA splicing by a yet unknown mechanism. Upon ER stress, RUVB-2 is degraded through an ubiquitin and p97/CDC-48-dependent mechanism, thereby allowing the ER-stress-specific transcription factors ATF6 and XBP-1 to activate the transcription of UPR^{ER} genes. Beyond unravelling a novel UPR^{ER} regulatory network, our data point toward the putative role of Reptin in non-conventional mRNA splicing. Our findings suggest that p97/CDC-48-induced degradation of target proteins plays an important role in the ER homeostasis control both, in the cytoplasm, to influence ERAD and to modulate UPR^{ER} gene transcription [13].

Materials and Methods

RNAi screen

The RNAi feeding screen was performed in liquid culture using EM2 animals and carried out as previously described with some modifications [4]. RNAi clones from the Worm ORFeome version 1.1 library [6] were grown overnight at 37°C in 96-well plates. Each RNAi plate included a positive control (Y37D8A.10 encoding for a signal peptidase identified in a preliminary screen or BC14636 worms fed with the L4440 empty vector) and a negative control (*gfp* RNAi). RNAi expression was induced with 1 mM IPTG for 1 h before bacteria were added to the L1 larvae. Adult worms were bleached,and the obtained L1 larvae (200) were added to each well of 96-well plates along with the induced bacteria and S-Medium, 50 μg/ml ampicillin, 1 mM IPTG buffer with a final well volume of 150 μl. The 96-well plates were incubated at 20°C with shaking. Forty-eight hours later, ER stress was induced by tunicamycin (0.5 μg/ml) for 16 h, and measurements were taken using the COPAS Biosort flow cytometer (Union Biometrica, Holliston, MA, USA). Experiments for each 96-well plate from the RNAi library were performed in duplicate. Fluorescence average value for each plate was calculated and used to calculate the individual RNAi fold change. Plates showing no fluorescence induction in the positive control, no fluorescence decrease in negative control, or a high fluorescence mean were discarded and retested.

COPAS measurements

The COPAS biosort analyzer was purchased from Union Biometrica (Holliston, MA, USA). Photomultiplicator tube control (PMT1) was set up at 600 so that the green fluorescence emission was not saturated in BC14636 worms exposed to tunicamycin (maximum signal) and still detectable in EM2 worms exposed to *gfp* RNAi (minimum signal). Plates were read through a ReFLx module. Raw data extracted from COPAS included worm axial length (time of flight),

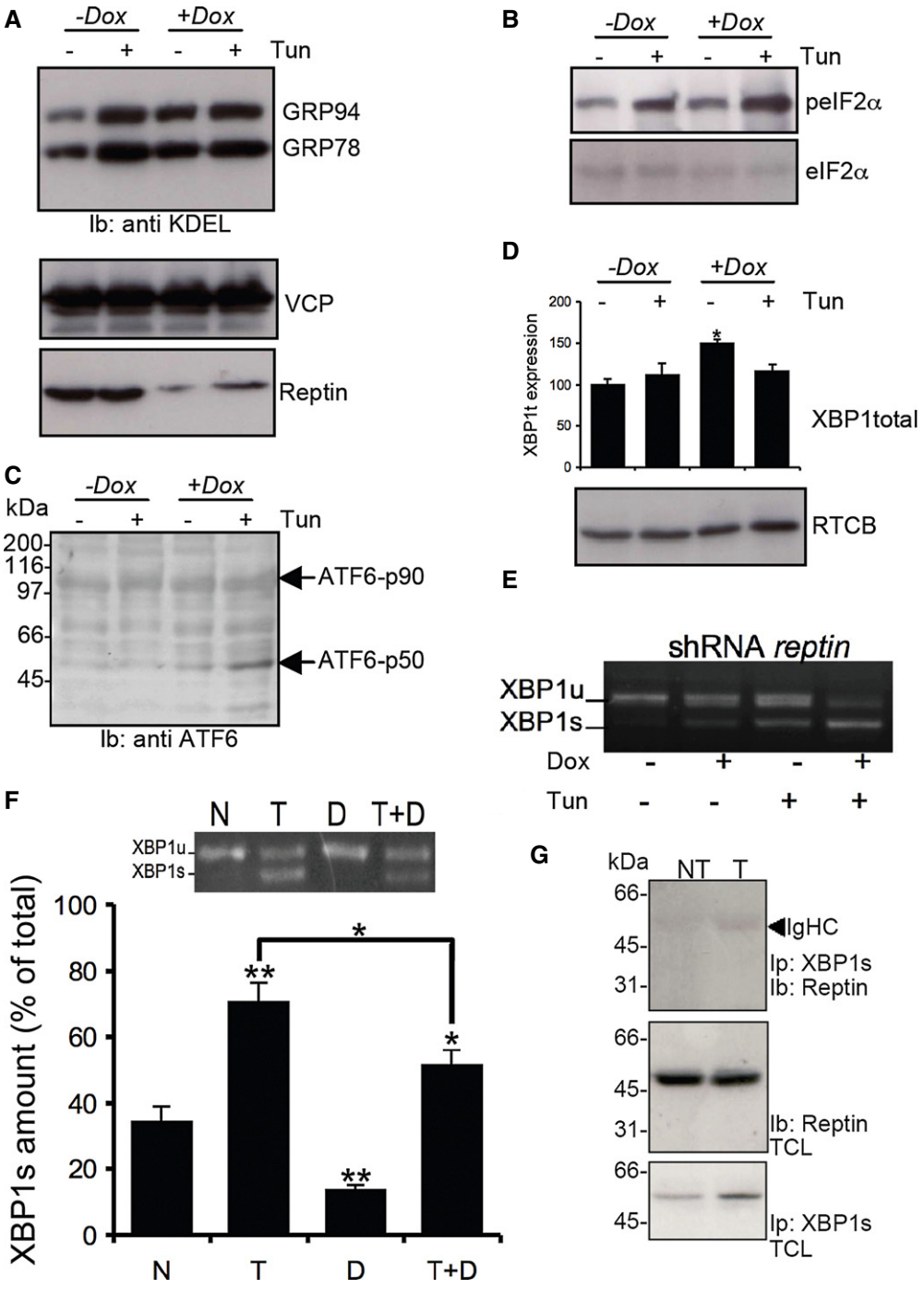

Figure 5. Reptin silencing enhances ATF6 and XBP1s activation.

A GRP78 and GRP94 expression was detected using anti-KDEL antibodies (top blot) in HuH7 cells treated or not with tunicamycin and/or doxycycline (Dox) to induce reptin silencing (bottom blot). Expression of p97 was also monitored (middle blot).

B eIF2α phosphorylation was monitored using specific antibodies (top blot) and reported to the total expression (bottom blot) in HuH7 cells treated or not with tunicamycin and/or doxycycline (Dox).

C ATF6 activation was monitored in the same experimental conditions using antibodies against the N-terminal domain of ATF6.

D Expression of unspliced XBP1 mRNA as determined by RT–PCR and expression of the XBP1s ligase RTCB as determined by immunoblot using anti-RTCB antibodies in HuH7 cells treated or not with tunicamycin and/or doxycycline (Dox).

E XBP-1 mRNA splicing as determined by RT–PCR under basal conditions or upon tunicamycin treatment (5 μg/ml for 16 h) in HuH7 cells subjected or not to doxycycline-induced *Reptin* silencing. Three independent experiments were performed, and a representative image is shown.

F HuH7 cells were treated either with DBeQ (20 μM, D), tunicamycin (2 μg/ml; T) or both for 4 h. XBP-1 mRNA splicing was determined by RT–PCR (Mean ± SD, $N = 3$). *P*-values were calculated using multiple *t*-test corrected using the Holm-Sidak method. *$P < 0.05$; **$P < 0.01$.

G HuH7 cells were treated with tunicamycin (2 μg/ml; T) for 1 h. XBP1s was immunoprecipitated, and the complex was immunoblotted with anti-Reptin antibodies (top blot). Total cell lysate (TCL) was immunoblotted with anti-Reptin (middle blot) or anti-XBP1s (bottom blot).

worm number (extinction) and fluorescence (green fluorescence emission). Raw data were processed as previously described [14] and used for quantitative analyses.

Supplementary information for this article is available online: http://embor.embopress.org

Acknowledgements
We thank Dr. R. Pedeux for help with the post-translational modifications of reptin, E Attebi and K Rebora for help with *C. elegans* screens, Drs E. Snapp and F. Schoenen for the ERSE::Tomato construct and DBeC, respectively, Dr. S. Mitani for the *cdc-48.1(tm544)* and *cdc-48.2(tm659)* strains. This work was funded by grants from "Institut National du Cancer" to EC and JR. EM was funded by a scolarship from Association Française contre les Myopathies.

Author contributions
EM, AAR, ST, KB, EC, JWD and NPL performed experiments. LG and DD developed the bioinformatics tools. MB supervised the proteomics analysis. JR and FP provided tools. EM, DD and EC coordinated the study. EM, MFZ, DD and EC wrote the manuscript.

Conflict of interest
The authors declare that they have no conflict of interest.

References

1. Ellgaard L, Helenius A (2003) Quality control in the endoplasmic reticulum. *Nat Rev Mol Cell Biol* 4: 181 – 191
2. Hetz C, Chevet E, Harding HP (2013) Targeting the unfolded protein response in disease. *Nat Rev Drug Discov* 12: 703 – 719
3. Mouysset J, Kähler C, Hoppe T (2006) A conserved role of *Caenorhabditis elegans* CDC-48 in ER-associated protein degradation. *J Struct Biol* 156: 41 – 49
4. Caruso ME, Jenna S, Bouchecareilh M, Baillie DL, Boismenu D, Halawani D, Latterich M, Chevet E (2008) GTPase-mediated regulation of the unfolded protein response in *Caenorhabditis elegans* is dependent on the AAA+ ATPase CDC-48. *Mol Cell Biol* 28: 4261 – 4274
5. Dantuma NP, Hoppe T (2012) Growing sphere of influence: Cdc48/p97 orchestrates ubiquitin-dependent extraction from chromatin. *Trends Cell Biol* 22: 483 – 491
6. Reboul J, Vaglio P, Rual JF, Lamesch P, Martinez M, Armstrong CM, Li S, Jacotot L, Bertin N, Janky R *et al* (2003) *Caenorhabditis elegans* ORFeome version 1.1: experimental verification of the genome annotation and resource for proteome-scale protein expression. *Nat Genet* 34: 35 – 41
7. Squiban B, Belougne J, Ewbank J, Zugasti O (2012) Quantitative and automated high-throughput genome-wide RNAi screens in *C. elegans*. *J Vis Exp* pii: 3448
8. Shen X, Ellis RE, Sakaki K, Kaufman RJ (2005) Genetic interactions due to constitutive and inducible gene regulation mediated by the unfolded protein response in *C. elegans*. *PLoS Genet* 1: e37
9. Lajoie P, Snapp EL (2011) Changes in BiP availability reveal hypersensitivity to acute endoplasmic reticulum stress in cells expressing mutant huntingtin. *J Cell Sci* 124: 3332 – 3343
10. Haurie V, Ménard L, Nicou A, Touriol C, Metzler P, Fernandez J, Taras D, Lestienne P, Balabaud C, Bioulac-Sage P *et al* (2009) Adenosine triphosphatase pontin is overexpressed in hepatocellular carcinoma and coregulated with reptin through a new posttranslational mechanism. *Hepatology* 50: 1871 – 1883
11. Christiano R, Nagaraj N, Fröhlich F, Walther TC (2014) Global Proteome Turnover Analyses of the Yeasts S. cerevisiae and S. pombe. *Cell Rep* 9: 1 – 7
12. Kosmaczewski SG, Edwards TJ, Han SM, Eckwahl MJ, Meyer BI, Peach S, Hesselberth JR, Wolin SL, Hammarlund M (2014) The RtcB RNA ligase is an essential component of the metazoan unfolded protein response. *EMBO Rep* 15: 1278 – 1285
13. Fessart D, Marza E, Taouji S, Delom F, Chevet E (2013) P97/CDC-48: Proteostasis control in tumor cell biology. *Cancer Lett* 337: 26 – 34
14. Dupuy D, Bertin N, Hidalgo CA, Venkatesan K, Tu D, Lee D, Rosenberg J, Svrzikapa N, Blanc A, Carnec A *et al* (2007) Genome-scale analysis of in vivo spatiotemporal promoter activity in *Caenorhabditis elegans*. *Nat Biotechnol* 25: 663 – 668

